

# Strangeness Production in Chemically Non-Equilibrated Parton Plasma

Peter Levai<sup>a1</sup> and Xin-Nian Wang<sup>b</sup>

<sup>a</sup>Research Institute for Particle and Nuclear Physics  
1525 Budapest 114. P.O.B. 49, Hungary

<sup>b</sup>Nuclear Science Division, M.S. 70A-3307  
Lawrence Berkeley Laboratory, Berkeley, CA 94720

**ABSTRACT:** Strangeness production was investigated during the equilibration of a gluon dominated parton plasma produced at RHIC and LHC energies. The time evolution of parton densities are followed by a set of rate equations in a 1-dimensional expanding system. The strangeness production will depend on the initial chemical equilibration level and in our case the parton densities will remain far from the full equilibrium. We investigate the influence of gluon fragmentation on final strangeness content.

## Introduction

Strangeness production was widely investigated during last decade as one of the possible quark-gluon plasma signatures [1]. To refresh our knowledge about the time dependence of strangeness content in case of parton gas, let us consider ultrarelativistic heavy ion collisions in the framework of pQCD-inspired parton interaction models [2, 3, 4]. In this framework, hard or semi-hard scatterings among partons dominate the reaction dynamics. They can liberate partons from the individual nucleons, thus producing large amount of transverse energy in the central region [5], and drive the initially produced parton system toward equilibrium [3, 6, 7].

Roughly speaking, ultrarelativistic heavy-ion collisions in a partonic picture can be divided into three stages: (1) During the early stage, hard or semi-hard parton scatterings, which happen on a time scale of about  $0.2 \text{ fm}/c$ , produce a hot and undersaturated parton gas. This parton gas is dominated by gluons and its quark content is far below the chemical equilibrium value. Interference and parton fusion also leads to the depletion of small  $x$  partons in the effective parton distributions inside a nucleus, reducing the initial parton

---

<sup>1</sup> The talk was presented by P. Levai on S'95 Conference, Tucson, Jan. 3-7 1995. E-mail: plevai@sunserv.kfki.hu

production [8]. (2) After two beams of partons pass through each other, the produced parton gas in the central rapidity region starts its evolution toward (kinetic) thermalization mainly through elastic scatterings and expansion. The kinematic separation of partons through free-streaming gives an estimate of the time scale  $\tau_{iso} \approx 0.5 - 0.7 \text{ fm} = c$  [7, 9], when local isotropy in momentum distributions is reached. (3) Further evolution of the parton gas toward a fully (chemically) equilibrated parton plasma is dictated by the parton proliferation through induced radiation and gluon fusion. This chemical equilibration can be described by a set of rate equations for gluons and quarks with different flavours. Due to the consumption of energy by the additional parton production, the effective temperature of the parton plasma cools down considerably faster than the ideal Bjorken's scaling solution. Therefore, the life time of the plasma is reduced before the temperature drops below the QCD phase transition temperature [7].

Strangeness production could also be divided into the above three different contributions in the history of the evolution of the parton system. However, here we will skip the very complicated description of steps (1) and (2) and simply we consider the result of the HIJING Monte Carlo code for these early stages. We will concentrate on strangeness production in stage (3), investigating the strangeness evolution and saturation. We describe the equilibration of the initially produced hot and undersaturated parton gas following Ref. [7]. For gluons we apply the result of an improved perturbative QCD analysis of Landau-Pomeranchuk-Migdale effect (see Ref. [10] and Ref. [11]).

In our analysis we include one more step of strangeness production, namely the gluon fragmentation. We assume a two step hadronization process at a certain critical temperature: (a) gluons decay into quark-antiquark pairs forming quark-matter from the parton gas; (b) the quarks and antiquarks will be redistributed forming colorless hadrons. For simplicity, we will use the well-known string breaking factors for estimating the different flavour yields in the gluon decay reaction ( $g \rightarrow q + \bar{q}$ ). However more work will be needed to find out the medium-dependent values of these factors. The hadron formation by quark-antiquark redistribution is beyond of the scope of our recent investigation. However, the strange/non-strange quark-pair ratio will not change in this type of hadronization. One can find a detailed description of such a hadronization mechanism in Ref. [12].

We will study the strangeness production during the parton evolution. We also discuss the influence of the uncertainties in the initial parton density on the final saturation level of different flavours. We investigate the extra strangeness yield of the gluon fragmentation and we compare the change of the strange/non-strange quark ratio in a chemically non-equilibrated parton system to a fully equilibrated one.

## Initial conditions: hot and undersaturated parton gas

The initial conditions for the time evolution of thermalized but chemically non-equilibrated parton gas can be obtained from one of the microscopical models. Currently there are many models for incorporating hard and semi-hard processes in hadronic and nuclear collisions [2, 3, 4]. Here we will use the result of the Hijing Monte Carlo model [2] to estimate the initial parton production at time,  $t_{iso}$ .

Since we are primarily interested in the chemical equilibration of the parton gas which has already reached local isotropy in momentum space, we shall assume that a parton distribution can be approximated by thermal phase space distribution with non-equilibrium fugacity :

$$f(k; T; \mu) = e^{u \cdot k - T} \mu^{\epsilon}; \quad (1)$$

where  $u$  is the four-velocity of the local comoving reference frame. When a parton fugacity  $\mu$  is much less than unity as may happen during the early evolution of the parton system, we can neglect the quantum corrections in Eq. (1) and write the momentum distributions in the factorized form,

$$f(k; T; \mu) = e^{u \cdot k - T} \mu^{\epsilon}; \quad (2)$$

Using this distribution in the comoving frame for a multi-component parton gas, one can obtain the total parton density, energy density and pressure as

$$n = n_g + \sum_i (n_{q_i} + n_{\bar{q}_i}) = (a_1 + \sum_i b_1(x_i)) \mu^{\epsilon} \quad (3)$$

$$\epsilon = \epsilon_g + \sum_i (\epsilon_{q_i} + \epsilon_{\bar{q}_i}) = (a_2 + \sum_i b_2(x_i)) \mu^{\epsilon} \quad (4)$$

$$P = P_g + \sum_i (P_{q_i} + P_{\bar{q}_i}) = \frac{1}{3} (a_3 + \sum_i b_2(x_i) b_3(x_i)) \mu^{\epsilon} \quad (5)$$

Here  $a_1 = 16 \cdot (3)^2 = 144$  and  $a_2 = a_3 = 8 \cdot 2 = 16$  for the Bose distribution of gluons. For fermions ( $i = u; d; s$ ) we introduce the parameter  $x_i = m_i/T$ . For massless light quark-antiquark pairs one obtains  $b_1(0) = 2 \cdot 9 \cdot (3)^2 = 108$ ,  $b_2(0) = 2 \cdot 7^2 = 98$  and  $b_3(0) = 1$ . For massive strange quark-antiquark pairs one can determine these factors exactly (see in Appendix). Here we investigate baryon symmetric systems, which means  $n_u = n_d = n_s$ . Since boost invariance has been demonstrated to be a good approximation for the initially produced partons [9], we can estimate the initial parton fugacities,  $\mu_g$ ;  $\mu_i$  and temperature  $T_0$  from

$$n_0 = \frac{1}{R_A^2} \frac{dN}{dy}; \quad \epsilon_0 = n_0 \frac{4}{3} k_B T_0; \quad (6)$$

where  $\langle k_{\perp} \rangle$  is the average transverse momentum. From HIJING one can obtain the initial values of the different gluon and quark fugacities. For different flavours the initial ratio is  $u : d : s = 2 : 2 : 1$ , approximately.

Table 1. shows these relevant quantities at the momentum  $p_{iso}$ , for Au + Au collisions at RHIC and LHC energies. One can observe that the initial parton gas is rather hot reflecting the large average transverse momentum. However, the parton gas is undersaturated as compared to the ideal gas at the same temperature. The gas is also dominated by gluons with its quark content far below the chemical equilibrium value. We should emphasize that the initial conditions listed here result from HIJING calculation of parton production through semi-hard scatterings. Soft partons, e.g., due to parton production from the color field [14], are not included.

Au + Au	RHIC	LHC
$p_{iso}$ (fm/c)	0.7	0.5
$\mu_0$ (GeV/fm <sup>3</sup> )	3.2	40
$n_0$ (fm <sup>-3</sup> )	2.15	18
$\langle k_{\perp} \rangle$ (GeV)	1.17	1.76
$T_0$ (GeV)	0.55	0.82
$\mu_g^0$	0.05	0.124
$\mu_u^0$	0.004	0.01
$\mu_d^0$	0.004	0.01
$\mu_s^0$	0.002	0.005

Table 1: Values of the relevant parameters characterizing the parton plasma at the momentum  $p_{iso}$ , when local isotropy of the momentum distribution is first reached.

## Master rate equations

In general, chemical reactions among partons can be quite complicated because of the possibility of initial and final-state gluon radiations. Interference effects due to multiple scattering inside a dense medium, i.e., LPM suppression of soft gluon radiation has to be taken into account. One lesson one has learned from LPM effect [10] is that the radiation between two successive scatterings is the sum, on the amplitude level, of both the initial state radiation from the first scattering and the final state radiation from the second one. Since the on-shell parton is space-like in the first amplitude and time-like in the second, the picture of a time-like parton propagating inside a medium in the parton cascades simulations [3] shall break down. Instead, we shall here consider both initial and final state radiations together associated with a single scattering

(to the leading order, a single additional gluon is radiated, such as  $gg \rightarrow ggg$ ), in which we can include LPM effect by a radiation suppression factor. The analysis of QCD LPM effect in Ref. [10] has been done for a fast parton traveling inside a parton plasma. We will use the results for radiation of thermal partons whose average energy is about  $T$ , since we expect the same physics to happen.

In order to permit the approach to chemical equilibrium, the reverse process, i.e., gluon absorption, has to be included as well, which is easily achieved making use of detailed balance. We consider only the dominant process  $gg \rightarrow ggg$ . Radiative processes involving quarks have substantially smaller cross sections in pQCD, and quarks are considerably less abundant than gluons in the initial phase of the chemical evolution of the parton gas. Here we are interested in understanding the basic mechanisms underlying the formation of a chemically equilibrated quark-gluon plasma, and the essential time-scales. We hence restrict our considerations to the dominant reaction mechanisms for the equilibration of each parton flavor. These are just four basic processes [15]:

$$gg \rightarrow ggg; \quad gg \rightarrow q_i \bar{q}_i; \quad (7)$$

Other scattering processes ensure the maintenance of thermal equilibrium ( $gg \rightarrow gg$ ;  $qq_i \rightarrow qq_i$ , etc.) or yield corrections to the dominant reaction rates ( $qq_i \rightarrow q_i gg$ , etc.).

Restricting to the reactions Eq. (7) and assuming that elastic parton scattering is sufficiently rapid to maintain local thermal equilibrium, the evolution of the parton densities is governed by the master equations [7]:

$$\partial_t (n_g u) = \frac{1}{2} \sigma_3 n_g^2 (1 - \frac{n_g}{n_g^*}) \times \left[ 2 \frac{1}{2} \sigma_2 n_g^2 (1 - \frac{n_{q_i}^2 n_g^2}{n_{q_i}^2 n_g^2}) \right]; \quad (8)$$

$$\partial_t (n_{q_i} u) = \partial_t (n_{\bar{q}_i} u) = \frac{1}{2} \sigma_2 n_g^2 (1 - \frac{n_{q_i}^2 n_g^2}{n_{q_i}^2 n_g^2}); \quad (9)$$

where  $n_g = n_y = n_g$  and  $n_{q_i} = n_{\bar{q}_i} = n_i$  denote the densities with unit fugacities,  $n_g = n_{q_i} = 1$ ,  $\sigma_3$  and  $\sigma_2$  are thermally averaged, velocity weighted cross sections,

$$\sigma_3 = \langle h(gg \rightarrow ggg) v_i \rangle; \quad \sigma_2 = \langle h(gg \rightarrow q_i \bar{q}_i) v_i \rangle; \quad (10)$$

In Eq. (9) we neglected the exchange between quark flavours, because generally the gluonic channel is dominant. We have also assumed detailed balance and a baryon symmetric matter,  $n_{q_i} = n_{\bar{q}_i}$ . If we neglect effects of viscosity due to elastic scattering [14, 16], we then have the hydrodynamic equation

$$\partial_t (\epsilon u) + P \partial_x u = 0; \quad (11)$$

which determines the evolution of the energy density.

For a time scale  $\tau_A$ , we can neglect the transverse expansion and consider the expansion of the parton plasma purely longitudinal, which leads to the Bjorken's scaling solution [17] of the hydrodynamic equation:

$$\frac{d''}{d} + \frac{'' + P}{''} = 0: \quad (12)$$

Evaluating this ultrarelativistic equation of motion by means of Eqs. (4)–(5) one obtains

$$\frac{''_g}{g} + 4 \frac{T}{T} + \frac{1}{3} \frac{''_g}{g} + \sum_i \left( \frac{''_i}{i} + 4 \frac{T}{T} D_n(x_i) + \frac{1}{1 + \frac{1}{3} b_3(x_i)} \frac{''_i}{i} \right) = 0 \quad (13)$$

where  $''_i = ''_{q_i} + ''_{\bar{q}_i}$  and  $D_n(0) = b_3(0) = 1$  for massless quark-antiquark pairs,  $D_n(x_s)$ ,  $b_3(x_s)$  for massive strange quark can be found in Appendix. Rewriting the rate equations Eqs. (7)–(8) in terms of time evolution of the parameters  $T(\tau)$ ,  $g(\tau)$  and  $''_i(\tau)$ , one obtains

$$\frac{''_g}{g} + 3 \frac{T}{T} + \frac{1}{3} = R_3 (1 - g) \quad (14)$$

$$\frac{''_i}{i} + 3 \frac{T}{T} D_n(x_i) + \frac{1}{1 + \frac{1}{3} b_3(x_i)} \frac{''_i}{i} = R_2^i \frac{n_g}{n_{q_i}} \quad (15)$$

where the density weighted reaction rates  $R_3$  and  $R_2^i$  are defined as

$$R_3 = \frac{1}{2} \sum_i n_g; \quad R_2^i = \frac{1}{2} \sum_i n_{q_i} \quad (16)$$

Notice that for a fully equilibrated system ( $g = \sum_i 1$ ), Eq. (13) corresponds to the Bjorken solution,  $T(\tau) = T_0 = (0 = \tau)^{1/3}$ . In Eq. (15)  $D_n(0) = 1$  and for  $D_n(x_s)$  see Appendix.

## Parton equilibration rates

To take into account of the LPM effect in the calculation of the reaction rate  $R_3$  for  $gg \rightarrow ggg$ , we simply impose the LPM suppression of the gluon radiation whose effective formation time  $\tau_{QCD}$  is much longer than the mean-free-path  $\lambda_f$  of multiple scatterings to each  $gg \rightarrow ggg$  process. In the mean time, the LPM effect also regularizes the infrared divergency associated with QCD radiation. However,  $R_3$  still contains infrared singularities in the gluon propagators. For an equilibrium system one can in principle apply the resummation technique developed by Braaten and Pisarski [18] to regularize the electric part of the propagators, though the magnetic sector still has to be determined by an unknown magnetic screening mass which can only be calculated non-perturbatively [19] up to now. Since we are dealing with a non-equilibrium

system, Braaten and Pisarski's resummation may not be well defined. As an approximation, we will use the Debye screening mass [13],

$$m_D^2 = \frac{6g^2}{2} \int_0^{\infty} k f(k) dk = 4 g_s T^2 g; \quad (17)$$

to regularize all singularities in both the scattering cross sections and the radiation amplitude.

The mean-free-path for elastic scatterings is

$$\lambda_g^{-1} = n_g \int_0^{\infty} dq_k^2 \frac{d_{el}^{gg}}{dq_k^2} = n_g \int_0^{\infty} dq_k^2 \frac{9}{4} \frac{2}{(q_k^2 + \frac{m_D^2}{2})^2} = \frac{9}{8} a_1 g_s T \frac{1}{1 + 8 g_s g}; \quad (18)$$

which depends very weakly on the gluon fugacity  $g$  [11].

The modified differential cross section for  $gg \rightarrow ggg$  has the form :

$$\frac{d_3}{dq_k^2 dy d^2k_\perp} = \frac{d_{el}^{gg}}{dq_k^2} \frac{dn_g}{dy d^2k_\perp} (f_{QCD}) \left( \frac{p_\perp}{s} k_\perp \cosh y \right); \quad (19)$$

where the second step-function accounts for energy conservation,  $s = 18T^2$  is the average squared center-of-mass energy of two gluons in the thermal gas and the LPM suppression factor was approximated by a  $\theta$ -function,  $(f_{QCD})$ , where  $f_{QCD} = \cosh y = k_\perp$  is the effective formation time of the gluon radiation in SU(3) [10]. We can complete part of these integrations:

$$R_3 = T = \frac{32}{3a_1} g_s g (1 + 8 g_s g)^2 I(g); \quad (20)$$

where  $I(g)$  is a function of  $g$ ,

$$I(g) = \int_0^{\frac{p_\perp}{s}} dx \int_0^{\frac{2}{D}} dz \frac{z^8}{(1+z)^2} \frac{\cosh^{-1} \left( \frac{p_\perp}{x} \right)}{x [x + (1+z)x_D]^2 \frac{4xz x_D}{9}} + \frac{1}{s^{\frac{2}{f}}} \frac{\cosh^{-1} \left( \frac{p_\perp}{x} \right)}{[1 + x(1+z)y_D]^2 \frac{4xz y_D}{9}}; \quad (21)$$

where  $x_D = \frac{2}{D} \frac{2}{f}$ ,  $y_D = \frac{2}{D} = s$  and the integral is evaluated numerically [11].

Note that in principle one should multiply the phase-space integral by  $1=3!$  to take into account of the symmetrization of identical particles in  $gg \rightarrow ggg$  as in Ref. [6]. However, for the dominant soft radiation we consider here, the radiated soft gluon does not overlap with the two incident gluons in the phase-space. Thus we only multiply the cross section by  $1=2!$ .

The quark equilibration rates  $R_{\frac{1}{2}}$  for  $gg \rightarrow q_i q_i$  can be also calculated, following the approximations of Ref. [7]. We introduce the thermal quark mass as a cutoff in the logarithmically divergent integrals:

$$M_{\frac{1}{2}}^2 = m_{0;i}^2 + g + \frac{1}{2} (u + d + s) \frac{4}{9} g_s T^2; \quad (22)$$

Here  $m_{0,i}$  notes the bare quark mass,  $m_{0,u} = m_{0,d} = 0, m_{0,s} = 150 \text{ M eV}$ .

The total cross section is dominated by the Compton diagrams. The cross section is the following for the process  $g g \rightarrow q \bar{q}_i$ :

$$\frac{d_i}{dt} = \frac{2}{3s} \log \frac{1+s}{1-s} \left[ 1 + \frac{1}{2} \frac{M_i^2}{s} \frac{M_i^4}{s^2} \right] + \frac{7}{4} \frac{31 M_i^2}{4 s} \quad (23)$$

where  $\frac{q}{1-4M_i^2/s}$ .

To obtain the total cross section approximately, we integrate over the gluon distributions and we insert the thermal gluon mass,  $M_i$ , and the average thermal  $hs_i = 18T^2$  into the cross section:

$$\frac{d_i}{dt} \approx \frac{9}{4} \frac{(2)}{(3)} \frac{d_i}{dt} \Big|_{M_i; hs_i=18T^2} \quad (24)$$

By means of Eq. (24) one can derive numerically the production rates  $R_{\frac{1}{2}} = 1-2 \frac{1}{2} n_g$  which will be used in Eq. (14)-(15) in the calculation of the time evolution.

## Evolution of the parton plasma

With the parton equilibration rates which in turn depend on the parton fugacity, we can solve the master equations self-consistently and obtain the time evolution of the temperature and the fugacities. The time dependence of  $T$ ,  $g$  and  $q_i$  are shown in Fig. 1 a, and Fig. 2 a, for initial conditions listed in Table I. at RHIC and LHC energies. We find that the parton gas cools considerably faster than predicted by Bjorken's scaling solution ( $(T)^3 = \text{const.}$ ) shown as dotted lines, because the production of additional partons approaching the chemical equilibrium state consumes an appreciable amount of energy. The accelerated cooling, in turn, slows down the chemical equilibration process, which is more apparent at RHIC than at LHC energies. Therefore, the parton system can hardly reach its equilibrium state before the effective temperature drops below  $T_c \approx 200 \text{ M eV}$  in a short period of time of 2-3 fm/c at RHIC energy. At LHC energy, however, the parton gas will be closer to its equilibrium and the plasma may exist in a deconfined phase for as long as 4-5 fm/c.

We note that the initial conditions used here are the results of the HIJING model calculation in which only initial direct parton scatterings are taken into account. Due to the fact that HIJING is a QCD motivated phenomenological model, there are some uncertainties related to the initial parton production, as listed in Ref. [7]. We can estimate the effect of the uncertainties in the initial conditions on the parton gas evolution by multiplying the initial energy and parton number densities at RHIC and LHC energies by a factor of 4. This

will increase the initial fugacities approximately by a factor of 4 at the same initial temperature. With these high initial densities, the parton plasma can evolve closer to an equilibrated gluon gas as shown in Fig. 1b, and Fig. 2b, however the system is still non-equilibrated and dominated by gluons. The light quarks and strange quarks remain far from the full chemical equilibrium.

Thus we can conclude that perturbative parton production and scatterings are very likely to produce a fully equilibrated parton plasma in ultrarelativistic heavy ion collisions at RHIC and LHC energies. The strangeness content will be far from the equilibrium, also.

## Gluon fragmentation

We have seen that during the parton evolution strangeness and the other quarks were not produced at equilibrium level. Thus the last possibility to get some more strangeness is the gluon fragmentation before hadronization. In an oversimplified model we can investigate the relative strangeness enhancement or suppression in the hadronization. We assume a two step hadronization process at a certain critical temperature: (a) gluons decay into quark-antiquark pairs forming quark-matter from the parton gas; (b) the quarks and antiquarks will be redistributed forming colorless hadrons.

For simplicity, we will use the well-known string breaking factors to estimate the different flavour yields in the gluon decay process ( $g \rightarrow q + \bar{q}_i$ ), namely  $f_u = f_d = 0.425$  and  $f_s = 0.15$ . Generally, in a hot and under-saturated parton gas these factors will not be valid automatically, but in lack of correct, temperature and parton density dependent values, here we will use the above numbers. Let us define the relative strangeness content by the strange/non-strange flavour ratio  $g_s$ :

$$g_s = \frac{n_s}{n_u + n_d} \quad (25)$$

One can determine easily this ratio  $g_s$  in the non-equilibrated parton gas before and after fragmentation and we can compare its value to a fully equilibrated quark-gluon plasma characterized by the same temperature. Fig. 1c, d, and Fig. 2c, d, show the results of our calculation at RHIC and LHC energies.

On Fig. 1c, full lines display the ratio  $g_s$  for the previously calculated gluon dominated non-equilibrium parton gas (smaller value,  $g_s = 0.25$  and marked as "Non-eq.") and for the fully equilibrated quark-gluon plasma (larger value,  $g_s = 0.45$  and marked as "Eq."). Gluon fragmentation, characterized by above values  $f_i$ , leads to the enhancement of the light quark flavours and the suppression of the strangeness. On Fig. 1c, after fragmentation  $g_s$  will drop in both

non-equilibrium (dotted line marked as "Fr-Non-eq" and  $g_s = 0.18$ ) and equilibrium cases (dashed line marked as "Fr-Eq" and  $g_s = 0.28$ ). Thus strangeness will be suppressed during hadronization in any case and any time step. Even if we consider 4 times higher initial parton fugacities (see Fig.1 d,) then we will have very much the same result as before. Moreover, the final  $g_s$  ratio will depend very weakly on the initial condition.

On Fig.2.c, we repeated the gluon fragmentation at LHC energy. We obtained an ~25% increase in strangeness comparing to the RHIC energy and an evolution which is slightly closer to the equilibrium ones. On Fig.2.d, the 4 times larger initial parton fugacities display a similar increase in strangeness, however the strangeness ratio will also drop during hadronization.

Our conclusions are the following: (a) before fragmentation  $g_s$  is far from its equilibrium value and it depends very strongly on the initial parton fugacities; (b) the above simple gluon fragmentation will decrease this  $g_s$  factor, suppressing the strangeness in a quark matter; (c) after fragmentation in equilibrium case  $g_s = 0.3$ , in non-equilibrium case  $g_s = 0.2$  at RHIC energy and  $g_s = 0.25$  at LHC energy.

This factor  $g_s$  is important, because after gluon fragmentation the above favour ratio will not change during the quark redistribution and it will determine the final strange/non-strange hadron ratio. The hadron formation via quark and antiquark redistribution is beyond of the scope of our recent investigation. One can find a detailed description of such a hadronization mechanism in Ref. [12] where at 200 GeV/n bombarding energy (CERN SPS) it was extracted  $g_s = 0.16$  for nucleon-nucleon and  $g_s = 0.255$  for S+ S collision.

## Conclusions

In this paper, we have calculated strangeness production in an equilibrating parton plasma, taking into account the evolution of the effective temperature and parton fugacities according to the solution of a set of rate equations. In the evaluation of the interaction rate  $R_3$  for induced gluon radiation, a color dependent effective formation time was used which reduces the gluon equilibration rate through LPM suppression of soft gluons.

We found that the thermal contribution during the parton equilibration with the current estimate of the initial parton density from HIJING Monte Carlo simulation are larger than the initial direct strangeness production, but the reached saturation level remains far from the full equilibrium at RHIC and LHC energies. The strangeness production depends on the initial condition of the parton evolution. If uncertainties in the initial parton production can increase the initial parton density, e.g., by a factor of 4, the secondary strangeness production will be larger, but even in this case it will not reach the total chemical equilibrium.

However, during hadronization the yield of light quarks can be much larger as the strange one. Thus the hadronization process may lead to a strangeness suppression. This conclusion very much depends on the fragmentation ratios. The strange/non-strange quark ratio will be also far from its equilibrium value during the partonic evolution. Moreover it could drop during hadronization and the non-equilibrium characteristic will be conserved.

## Appendix

For massive partons we have used the following expressions:

$$b_1(x_i) = 2 \frac{d_i}{2^2} \sum_{n=1}^3 (1)^{n+1} \frac{1}{nx_i} K_2(nx_i) \quad (26)$$

$$b_2(x_i) = 2 \frac{d_i}{2^2} \sum_{n=1}^4 (1)^{n+1} \left[ \frac{3}{(nx_i)^2} K_2(nx_i) + \frac{1}{(nx_i)} K_1(nx_i) \right] \quad (27)$$

$$b_3(x_i) = \frac{\sum_{n=1}^1 (1)^{n+1} \frac{1}{(nx_i)^2} K_2(nx_i)}{\sum_{n=1}^1 (1)^{n+1} \left[ \frac{1}{(nx_i)^2} K_2(nx_i) + \frac{1}{3} \frac{1}{(nx_i)} K_1(nx_i) \right]} \quad (28)$$

$$D_n(x_i) = \frac{\sum_{n=1}^1 (1)^{n+1} \left[ \frac{1}{(nx_i)} K_2(nx_i) + \frac{1}{3} K_1(nx_i) \right]}{\sum_{n=1}^1 (1)^{n+1} \frac{1}{(nx_i)^2} K_2(nx_i)} \quad (29)$$

$$D_{n'}(x_i) = \frac{\sum_{n=1}^1 (1)^{n+1} \left[ \frac{1}{(nx_i)^2} K_2(nx_i) + \frac{5}{12} \frac{1}{(nx_i)} K_1(nx_i) + \frac{1}{12} K_0(nx_i) \right]}{\sum_{n=1}^1 (1)^{n+1} \left[ \frac{1}{(nx_i)^2} K_2(nx_i) + \frac{1}{3} \frac{1}{(nx_i)} K_1(nx_i) \right]} \quad (30)$$

with  $x_i = m_i/T$  and  $d_i = 6$ . The factor  $(1)^{n+1}$  is connected to fermions.

## Acknowledgments

P.L. would like to thank T.S. Biro, B. Kämpfer and J. Zimanyi for helpful discussions. P.L. was supported by the Hungarian Science Fund, OTKA No. T 014213. X.-N.W. was supported by the Director, Office of Energy Research, Division of Nuclear Physics of the Office of High Energy and Nuclear Physics of the U.S. Department of Energy under Contract No. DE-AC 03-76SF 00098 and DE-FG 05-90ER 40592. P.L. and X.-N.W. were also supported by the U.S.-Hungary Science and Technology Joint Fund J.F.No. 93B/378.

## References

- [1] J. Rafelski, Phys. Rep. 88 (1982) 331; P. Koch, B. Muller, J. Rafelski, Phys. Rep. 142 (1986) 167; QM '91 Conference, Nucl. Phys. A 544 (1992) 1; QM '93 Conference, Nucl. Phys. A 566 (1994) 1.;
- [2] X.-N. Wang and M. Gyulassy, Phys. Rev. D 44, 3501 (1991); Comp. Phys. Commun. 83, 307 (1994).
- [3] K. Geiger and B. Muller, Nucl. Phys. B 369, 600 (1992); K. Geiger, Phys. Rev. D 47, 133 (1993).
- [4] H. J. Moehring and J. Ranft, Z. Phys. C 52, 643 (1991); P. Aurenche, et al., Phys. Rev. D 45, 92 (1992). P. Aurenche, et al., Comp. Phys. Commun. 83, 107 (1994).
- [5] J.P. Blaizot, A.H. Mueller, Nucl. Phys. B 289, 847 (1987); K. Kajantie, P.V. Landsho and J. Lindfors, Phys. Rev. Lett. 59, 2517 (1987); K. J. Eskola, K. Kajantie and J. Lindfors, Nucl. Phys. B 323, 37 (1989); K. J. Eskola, K. Kajantie and J. Lindfors, Phys. Lett. B 214, 613 (1989).
- [6] E. Shuryak, Phys. Rev. Lett. 68, 3270 (1992); E. Shuryak and L. Xiong, Phys. Rev. Lett. 70 2241 (1993); L. Xiong and E. Shuryak, Phys. Rev. C 49, 2207 (1994).
- [7] T. S. Biro, E. van Doo, B. Muller, M. H. Thoma, and X.-N. Wang, Phys. Rev. C 48, 1275 (1993).
- [8] S. J. Brodsky and H. J. Lu, Phys. Rev. Lett. 64, 1342 (1990); K. J. Eskola, J. Qiu and X.-N. Wang, Phys. Rev. Lett. 72, 36 (1994); X.-N. Wang and M. Gyulassy, Phys. Rev. Lett. 68, 1480 (1992).
- [9] K. J. Eskola and X.-N. Wang, Phys. Rev. D 49, 1284 (1994).
- [10] M. Gyulassy and X.-N. Wang, Nucl. Phys. B 420, 583 (1994); X.-N. Wang, M. Gyulassy and M. Plum er, LBL-35980, hep-ph/9408344.
- [11] P. Levai, B. Muller, X.-N. Wang, LBL-36594, hep-ph/9412352.
- [12] T. S. Biro, P. Levai, J. Zimanyi, Phys. Lett. B 347 6 (1995); T. S. Biro, P. Levai, J. Zimanyi, hep-ph/9504203 and see this Proceedings.
- [13] T. S. Biro, B. Muller, and X.-N. Wang, Phys. Lett. B 283, 171 (1992).
- [14] K. J. Eskola and M. Gyulassy, Phys. C 47, 2329 (1993).
- [15] T. Matsui, B. Svetitsky, and L. McLerran, Phys. Rev. D 34, 783 (1986).
- [16] P. Danielewicz and M. Gyulassy, Phys. Rev. D 31, 53 (1985); A. Hosoya and K. Kajantie, Nucl. Phys. B 250, 666 (1985); S. Gavin, Nucl. Phys. A 435, 826 (1985).
- [17] J. D. Bjorken, Phys. Rev. D 27, 140 (1983).
- [18] E. Braaten and R. D. Pisarski, Nucl. Phys. B 337, 569 (1990).
- [19] T. S. Biro and B. Muller, Nucl. Phys. A 561, 477 (1993).
- [20] J. F. Gunion and G. Bertsch, Phys. Rev. D 25, 746 (1982).

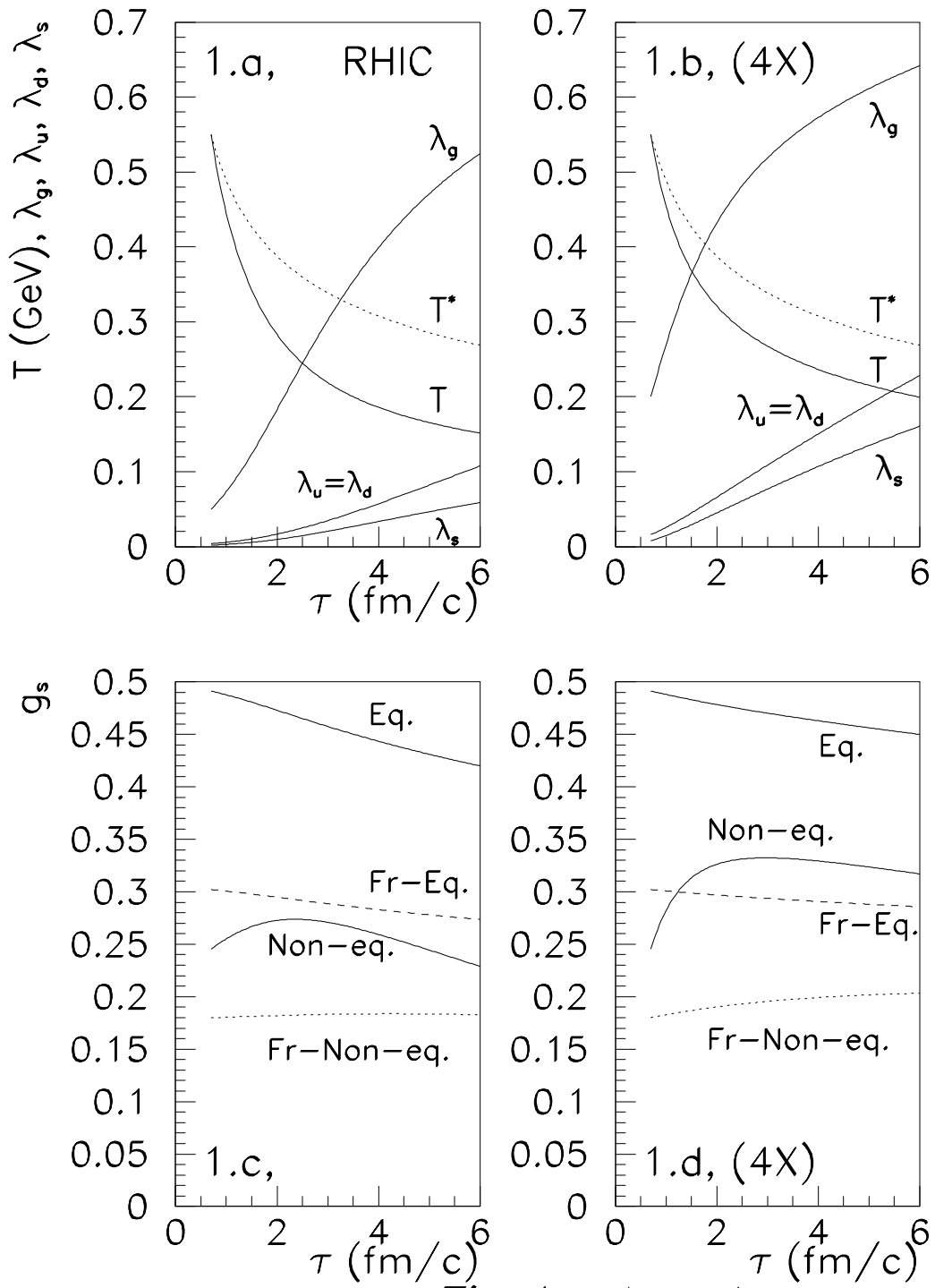


Fig. 1.a,b,c,d,

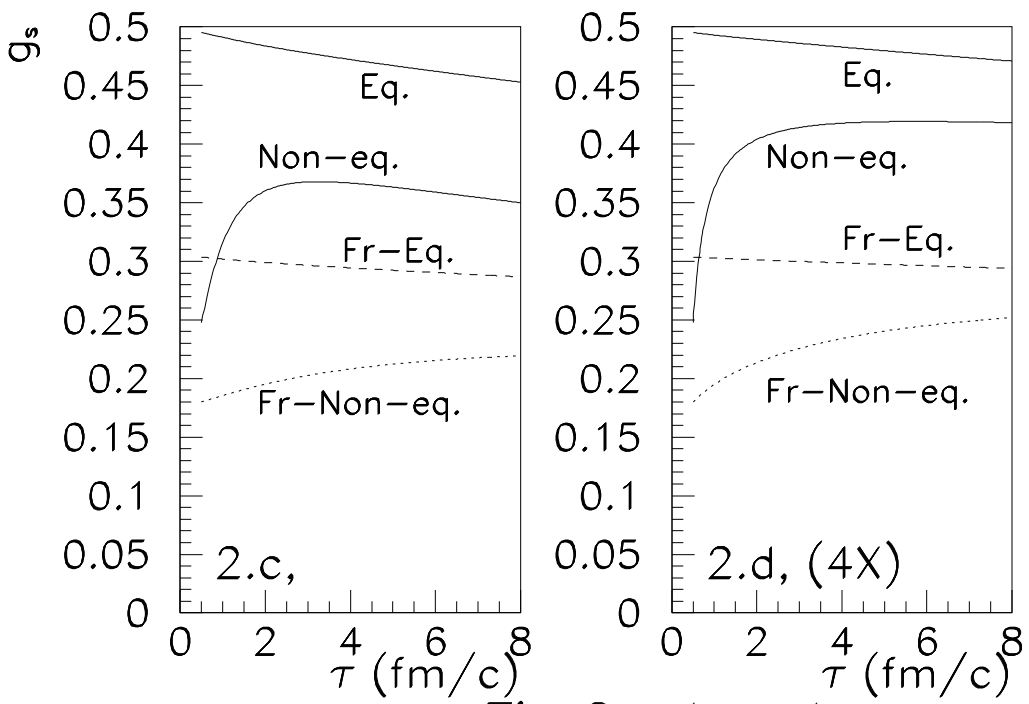
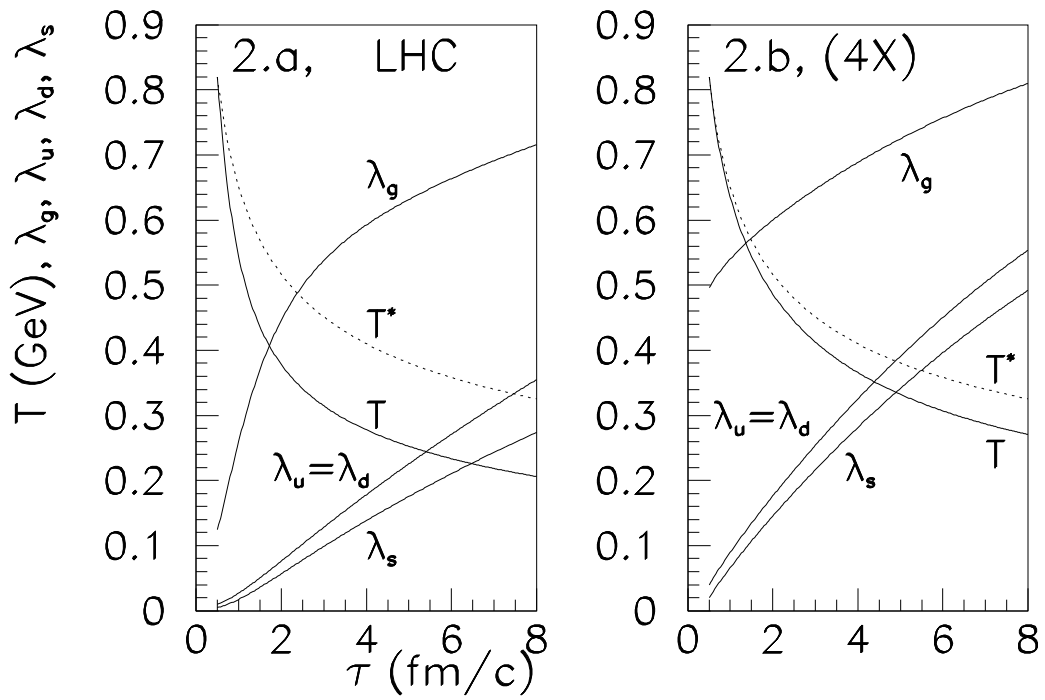


Fig.2.a,b,c,d,